Drag reduction in co-current down flow packed column using xanthan gum

Iyyaswami Regupathi*, Ponnan Ettiyappan JagadeeshBabu*, M. Chitra,
and Thanapalan Murugesan***,†**

*Department of Chemical Engineering, National Institute of Technology Karnataka, Mangalore 575 025, India
**Department of Chemical Engineering, A. C. College of Technology, Anna University, Chennai 600 025, India
***Chemical Engineering Department, Universiti Teknologi PETRONAS,
Bandar Seri Iskandar, 31750, Tronoh, Perak, Malaysia

Abstract−Drag reduction is one of the most important techniques for reducing energy consumption in a packed bed contactor. The present work involves an experimental investigation on flow regime transition for air-water system with and without drag reducing agent (DRA), two-phase pressure drop, friction factor and drag reduction using xanthan gum as DRA. Drag reduction was quantified from the two-phase pressure drop data. Based on the present observations it was found that the percentage drag reduction increases with an increase in the concentration of DRA and it is only effective in the range of 300 ppm to 800 ppm. The experimental results indicate that a maximum of 80% drag reduction was achievable using xanthan gum (800 ppm) as DRA. Furthermore, the experimental data were validated with the available literature correlations.

Key words: Drag Reduction, Packed Bed Down Flow, Two-phase Friction Factor and Xanthan Gum

INTRODUCTION

Three-phase packed bed reactors with co-current flow of gas and liquid are extensively utilized in chemical, petrochemical, biochemical and waste water treatment processes for many contacting purposes, such as gas absorption, gas absorption accompanied by a chemical reaction, and heterogeneous catalytic reactions. The co-current mode of operation is usually preferred over the countercurrent mode when there is no significant difference in the mean concentration driving force offered by the two phases. The reason for this lies in the additional advantages of the co-current mode, such as no limitation on gas and liquid throughputs (no flooding), offering a wide range of operable flow rates and a low pressure drop as compared with countercurrent operation. Also, the liquid back mixing is a more prominent disadvantage in the up-flow configuration than in the down-flow configuration in packed columns. The main advantage of the columns operating in the co-current down flow of the two phases is the possibility of using high flow rates without causing the onset of flooding in the column.

A phenomenon that is always an undesirable factor in packed bed co-current down flow contactors is the high axial pressure gradient, which results in substantial energy consumption per unit volume of liquid throughput. Turbulent flows occur in the boundary layer near solid surfaces where the associated friction increases as the flow velocity increases. The energy losses due to turbulence friction can be of very high magnitude, which requires further attention for minimization. Drag reduction is a phenomenon by which a small amount of additives, e.g. a few parts per million, can greatly reduce the turbulent friction factor of a fluid. The aim for the drag

reduction study is to improve the fluid-mechanical efficiency using active agents, known as drag reducing agents (DRA) named as the "Toms effect" [1].

Drag can be reduced by using diluted polymers, surfactants, micro bubble and compliant coating over a solid surface. Though surfactants and polymer additives offer almost 80% drag reduction, the former needs some higher degree of concentration than polymer solution [2]. During late fifties and early sixties, the effect of dilute polymer solutions on drag reduction was actively investigated. Lumley [3,4] defined drag reduction as the reduction of skin friction in turbulent flow below that of pure liquid. Form the literature it was concluded that the polymer solution can produce drag reduction only when flow remains turbulent. After Toms discovered turbulent drag reduction by polymer additives, many theoretical, experimental and numerical studies were conducted to explain the mechanism of polymer drag reduction. Two principal concepts have been suggested to explain the phenomenon of drag reduction by polymers: one is a mechanism based on the extensional viscosity and the other is that based on the elastic theory.

Studies on the drag reduction technologies, percentage drag reduction and friction factor are of great interest from the industrial point of view. In particular, drag reduction studies on packed columns are very much useful to reduce mechanical energy losses, which reduces the cost associated with transport of fluids like pumping, thus reducing the overall operating costs. The knowledge of flow regimes in a packed bed column, for a desired set of flow conditions, liquid properties viz., viscosity, density and surface tension and packing geometry, is essential for the proper design and successful scale-up of packed columns. The flow regimes in a packed bed down flow column have a significant influence on the design variables viz., pressure drop, liquid holdup, interfacial area and mass transfer coefficients. The mixing characteristics of the contacting phases and their

---

†To whom correspondence should be addressed.
E-mail: murugesan@petronas.com.my

transport properties in the column are more dependent on the operating flow regime in packed bed column which largely depends on the mass flow rate of gas-liquid phases, size and shape of the particles, bed voidage and physical properties of liquids.

Several studies have been conducted to determine the extent of drag reduction for different polymers in different systems. The dependency of drag reduction on various factors, including polymer molecular weight, polymer concentration and temperature, have been investigated by many authors [5-8]. Based on the literature review, it was found that the effect of xanthan gum as drag reducing agent in co-current air-water down flow through a packed column has not been reported till date. For the present work, it is proposed to use xanthan gum as drag reducing agent and to study its effect on flow regime transition, friction factor and drag reduction in co-current air-water down flow through a packed column.

EXPERIMENTAL SETUP
AND COLUMN OPERATION

1. Experimental Setup

The experimental setup consists of a Perspex column of 1.9 m in height and 0.115 m internal diameter. Fig. 1 shows the schematic representation of the packed column used for the present work. The column dimensions and particle dimensions are given in Table 1. At the top of the packed column a gas-liquid distributor was placed to ensure the regular and uniform distribution of air-liquid mixture inside the testing section. In the top gas-liquid distributor, liquid inlet was connected axially through solenoid valve and gas inlet was connected horizontally. A separate gas-liquid separator was provided at the bottom of the column to have proper separation of two
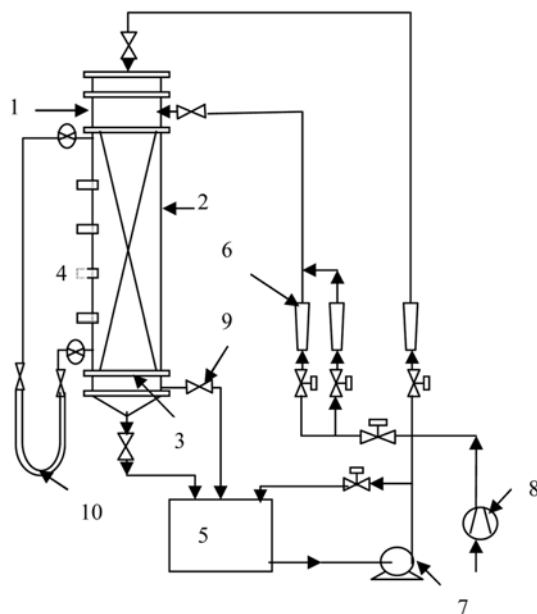

Fig. 1. Schematic view of experimental setup.
1. Gas-liquid distributor　　6. Rotameter
2. Testing section　　　　　　7. Centrifugal pump
3. Gas-liquid separator　　　　8. Compressor
4. Manometer tapping　　　　　9. Solenoid valve
5. Liquid storage tank　　　　 10. Manometer

Table 1. Column dimension and particle specifications

Effective packing height	0.8 m
Column diameter	0.115 m
Sphericity	1
Particle shape	Spherical shape
Particle type	Non porous glass beads
Bed voidage	0.386
Particle diameter	0.01605 m

Table 2. Physical properties of xanthan gum solution

Concentration	Density (kg/m^3)	n	K (kg/m s^{2-n})
300 ppm	1000.3	0.9445	0.00189
400 ppm	1000.4	0.9225	0.00232
600 ppm	1000.6	0.8945	0.00349
800 ppm	1000.8	0.8542	0.00632

different phases, where the separated liquids were re-circulated back to the column. The flow rates of two different phases (gas and Liquid) were measured using a calibrated rotameter. Liquid was pumped by a centrifugal pump and the flow rates were controlled with a gate valve, and compressed air was pumped into the column through the surge tank and then through the calibrated rotameter.

2. Measurement of Liquid Properties

The liquids used in this present work were water and water+xanthan gum solution of different concentration (300, 400, 600 and 800 ppm). The mixture behaves as a low shear thinning solution. Sine the liquid system used in this study exhibits a thyrotrophic nature, the basic properties like density and viscosity were measured using drop weight method (specific gravity bottle) and Haake viscometer (model VT 181), respectively, where the shear rate for various applied shear stresses was measured. The flow consistency index 'k' and flow behavior index 'n' were evaluated using the power law model which is given in Table 2.

3. Column Operation

3-1. Mode of Operation of Column

The column was operated under co-current down flow mode by allowing liquid and gas through the gas-liquid distributor located at the top of the column. Eight different manometer tapings were used in the column to measure the pressure drop at various positions across the length of the column. During operation the pressure drop was measured by a U-tube manometer for different phase flow rates. Initially, the experiments were carried out using an air-water system without DRA, and then it was extended with the addition of suitable xanthan gum (DRA) of different concentrations ranging from 300 to 800 ppm and air-Newtonian liquid systems (glycerol, ethylene glycol of different concentration) (JagadeeshBabu et al. [9]). Apart from the pressure drop data, another important hydrodynamic variable, flow regime was measured by visual method and compared with pressure drop method.

3-2. Measurement of Two Phase Friction Factor and Drag Reduction

A simple U-tube mercury manometer was used to measure the pressure drop across the testing section. Both ends of the manometer were initially connected to a gas-liquid separator and then con-

nected to the pressure tapings. Before taking readings from the manometer, care was taken to ensure that the limb of the manometer was filled with the same column liquid and that the limb was free from any gas bubbles that might interfere with the manometer readings. From the manometer reading the two phase pressure drop was measured. The drag reduction DR was calculated as below:

$$\% \ DR = (\Delta P_w - \Delta P_{DRA}) \times 100 / \Delta P_w \qquad (1)$$

RESULTS AND DISCUSSION

The knowledge of flow patterns plays a major role in determining the degree of drag generated in the packing, where the flow pattern purely depends on the fundamental variables like liquid properties such as viscosity, density and surface tension and packing geometry.

1. Flow Regimes and Flow Regimes Transition

Knowledge of the flow regime plays a vital role in the design of packed bed down-flow reactor. These flow patterns give a basic idea about bubble dynamics during gas-liquid interactions, which occurs between the stationary solid bed during column operation. The flow regime and flow regime transition plays a significant role in determining the hydrodynamic variables like pressure drop and corresponding phase holdup. In this present study, water is used as the liquid system and air is used as the gas medium. In general, flow patterns can be measured either by visual observation or by pressure drop method.

In this present study, visual observation was used to identify different flow regimes, and further it was confirmed by using the pressure drop method. Initially, the column was operated at low gas and liquid flow rate, where the liquid starts to trickle over the particle and the gas flows through the available pores. In this flow regime gas is considered as a continuous phase and liquid as discontinuous phase. Furthermore, with a moderate increase in the gas flow at constant liquid flow rate and vice versa, the drag force between the gas-liquid interface increases, which leads to the accumulation of small liquid droplets as discontinuous liquid rich zone traveling

downward causing a pulse regime. At high gas-liquid mass flow rate, the gas becomes discontinuous and liquid becomes continuous leading to dispersed bubble flow regime.

Visually observed flow regime data were plotted to identify the flow regime boundary between the three different flow patterns. Liquid mass velocity 'L' in kg/m²s as abscissa is plotted against gas mass velocity 'G' in kg/m²s. Fig. 2 shows the flow regime map for air water system without drag reducing agent. Three different flow patterns were observed: trickle flow, pulse flow and dispersed bubble flow. A C-shaped transition boundary was observed between different flow patterns. The flow patterns and flow regime boundaries (C-shape curve) observed in this study were compared with the Trivizadakis et al. [10] flow map (6mm-dia, 0.36-voidage, air-water) which showed good agreement.

In a single phase flow through a fixed bed column, the operating flow regimes are normally classified as laminar and turbulent, which is generally characterized by a single dimensionless group in the form of the Reynolds number with the established boundary conditions. But in the case of fixed bed gas-liquid-solid columns, the dynamic behavior is more complex due to the complex interactions between the contacting phases. The flow patterns in a down-flow packed bed contactor depends on the mass flow rate of the individual phases, size and shape of the particles, bed voidage and the physical properties of the liquid systems used. For establishing a generalized flow boundary equation between different flow patterns, two dimensionless parameters 'X' and 'Y' proposed by Charpentier and Favier [11] were used.

$$X = [(Fr)_l \ (D_p / D_c) \ \varepsilon^{-1}] \ \psi \qquad (2)$$

$$Y = [(Fr)_g / (Fr)_l \ (\varphi_s D_p / D_c)^{0.75} \ \varepsilon^{-1}] / \psi \qquad (3)$$

Where, $\Psi = [(\sigma_w / \sigma_l) \ (\mu_l / \mu_w) \ (\rho_w / \rho_l)^2]^{0.33} \qquad (4)$

To study the effect of drag reducing agent on flow boundary, a known quantity of xanthan gum (DRA) was added to water and the mixture was used as liquid phase, and the flow patterns were visually
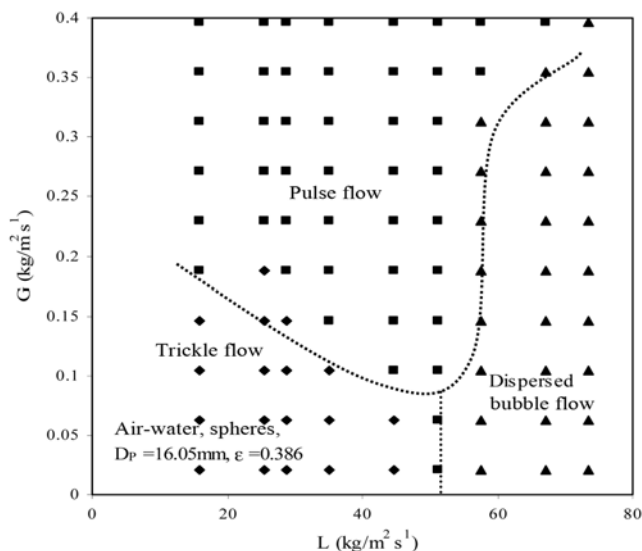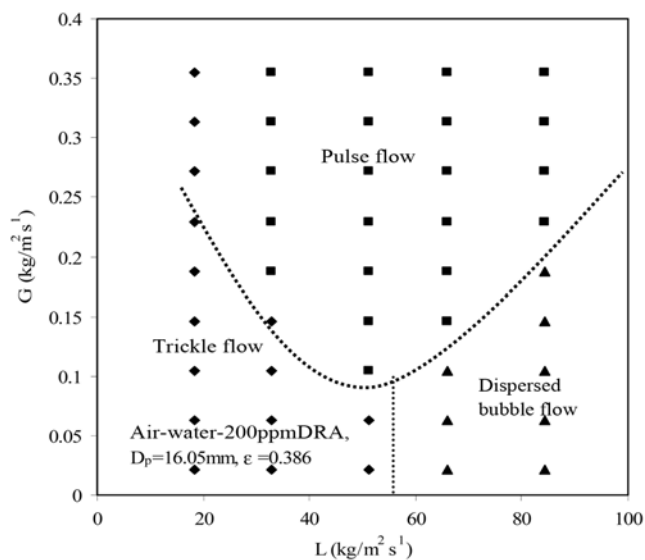

Fig. 2. Flow regime map for air-water system.

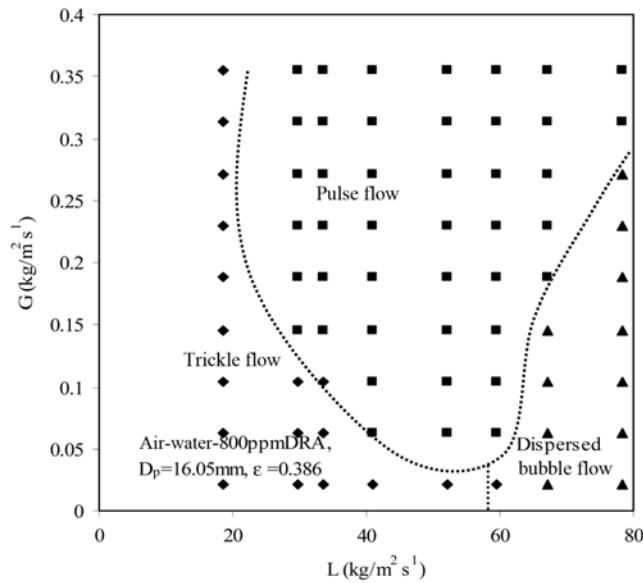Fig. 3. Flow regime map for air-water-xanthan gum system (300 ppm).

Fig. 4. Flow regime map for air-water-xanthan system (800 ppm).

Table 3. Boundary values for different flow regime as per equation (2 and 3)

Flow regime	Transition range of X and Y
Trickle flow	$Y<6\times10^{-8} X^{-1.587}$
	$X<4.16\times10^{-4}$
Trickle to pulse flow	$Y>6\times10^{-8} X^{-1.587}$
	$X<4.16\times10^{-4}$
Trickle flow to dispersed bubble flow	$X>4.16\times10^{-4}$
Dispersed bubble flow	$Y<2.32\times10^{5} X^{-2.147}$
	$X>4.16\times10^{-4}$
Dispersed bubble flow to pulse flow	$Y>2.32\times10^{5} X^{-2.147}$
	$X>4.16\times10^{-4}$

observed [12]. Figs. 3 and 4 show the flow regime transition map for air-water+xanthan gum system with xanthan gum concentration of 300 and 800 ppm, respectively. Figs. 3 and 4 indicate that DRA delays the onset of pulse flow or dispersed flow from trickle flow. Pressure drop reduction occurs in almost all flow pattern configurations. Oliver et al. [13] also reported that with the addition of DRA, the interfacial shear stress decreases sharply and the flow pattern transition is altered. The boundary conditions for the various flow transitions were estimated by using the present experimental data which is listed in Table 3.

Changes in the flow regime map for air-water+xanthan system from air-water system is mainly due to the changes in liquid density, viscosity and surface tension. Figs. 3 and 4 show the horizontal shift in boundary towards the right and also a slight upward shift, which may be attributed to the change in the viscosity of the solution. It was obvious that a shift from trickle flow to pulse flow occurred at high gas and liquid flow rates for the air-water+xanthan system. A slight right shift was also observed for 800 ppm compared to 300 ppm due to further increase in liquid viscosity. From Figs. 3 and 4 it was observed that the total shift in the boundary transition curve depends on the system properties which in turn depends

on the degree of drag changes occurring inside the column. In other words, changes in the flow regime map give the basic idea about the effect of xanthan gum on the drag reduction.

2. Drag Coefficient

Drag is the force offered by the fluid on the solid in the direction of flow. This drag is a function of the resistive force offered by the dynamic liquid and dynamic gas on their interaction and also the resistive force offered by the stationary solid phase. In the present study, uniform spherical particles were used as a packing material. The deviation in the drag coefficient under pure gas-water system and air-water+xanthan gum was analyzed. Deviations in uniformity of voidages were observed near the walls of the column which were normally accounted in the wall effects. The effect of Reynolds number on drag coefficient under both conditions was analyzed. The drag coefficient and modified Reynolds number were calculated as follows [14].

$$\text{Drag Coefficient} \qquad C_D = \frac{4\Delta P}{3L\rho_l(D_p)^n V^{2-n}(1-\varepsilon)} \qquad (5)$$

$$\text{Modified Reynolds Number } (\text{Re})_M = \frac{(D_p)^n (V)^{2-n}\rho_l\varepsilon}{6(1-\varepsilon)K} \qquad (6)$$
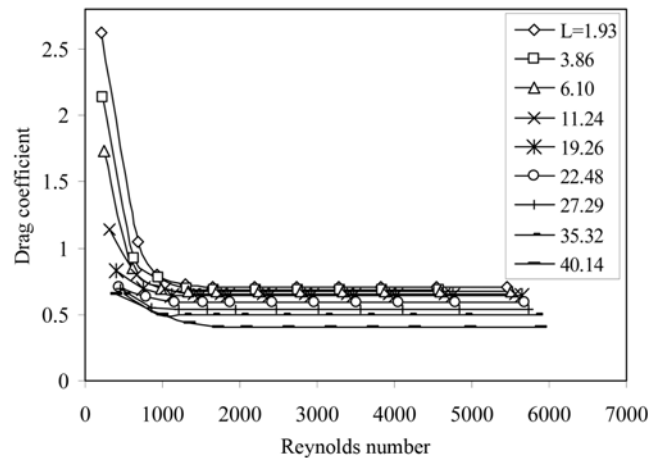

Fig. 5. Effect of Reynolds number on drag coefficient for air-water system.
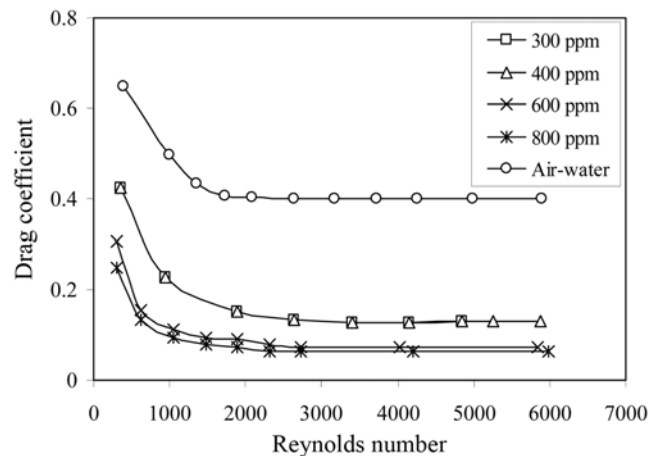

Fig. 6. Effect of xanthan concentration on drag coefficient at different Reynolds number.

From Fig. 5 it was observed that the drag coefficient decreases as the Reynolds number increases. The drag coefficient decreases sharply for a particular value of Reynolds number and then it stays almost constant. These results are supported by the previous literatures that drag coefficient decreases as Reynolds number increases. Fig. 6 shows the effect of drag coefficient for various concentrations of xanthan gum in water: 300, 400, 600 and 800 ppm. The addition of xanthan gum has a significant reduction in drag coefficient. As observed in the air-water system the drag coefficient reduces as the Reynolds number increased. Form Fig. 6 it was also observed that the drag coefficient for the air-water+xanthan system is low compared to the air-water system. Furthermore, a higher magnitude of drag reduction was observed with increase in xanthan gum concentration in water. Maximum reduction in drag coefficient was observed for 800 ppm. The drag coefficient is indirectly proportional to the DRA concentration. But as the concentration of xanthan gum reaches a maximum value of 800 ppm, the variation in the drag coefficient reduces, since the variation in the liquid properties reaches a constant value.

3. Friction Factor

In a packed bed down-flow contactor, the friction factor is one of the governing transport properties which play a major role. Tulin [15] proposed that at high strain rates the polymer chain (xanthan gum) tends to elongate along the principal strain rate axis, which results in larger extensions. As the elongation viscosity increases, the large scale bursts and sweeps in the wall layer, where flows are inhibited, thus reducing the friction. The effects of operating variables on friction factor were studied using both air-water system and air-water+xanthan system. The friction factor was calculated as follows:

$$\text{Friction Factor (f)} = \frac{\Delta P \varepsilon^3}{\rho_l (D_p)^n V^{2-n}(1-\varepsilon)L} \tag{7}$$

From the experimental data it was observed that, for each liquid flow rate, the friction factor decreases with increasing gas flow rate. Fig. 7 shows the relation between friction factor and Reynolds number for different mass velocity of water. The graph shows that the friction factor is high at low liquid mass velocity compared to higher
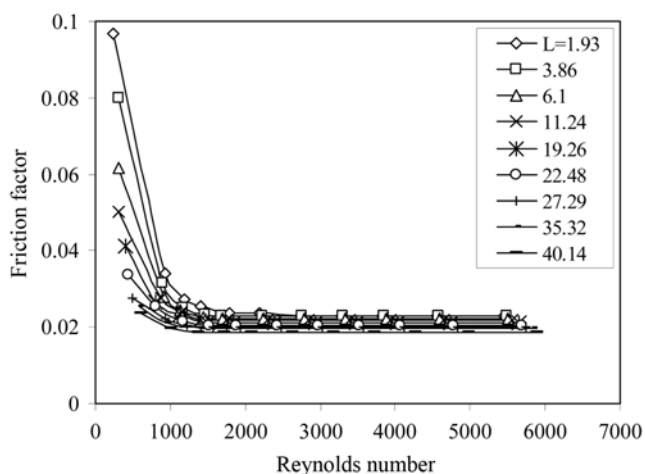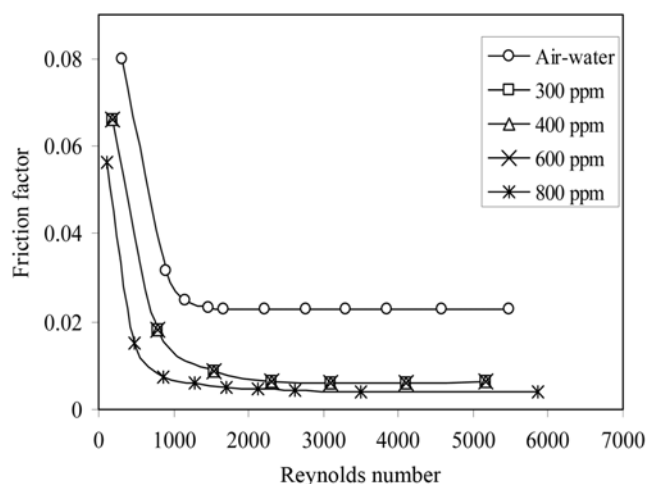

Fig. 8. Effect of xanthan concentration on friction factor at different Reynolds number.

liquid mass velocity. This could be attributed to the decrease in the friction between the solid-liquid interphase due to high turbulence. For low liquid mass velocity, friction is in higher order, resulting in substantial energy losses.

Fig. 8 shows the effect of various xanthan gum concentrations on friction factor. From the graph it was observed that the friction factor is more in case of pure water, and the friction factor decreases as the concentration of xanthan gum increases. With increase in polymer concentration, the solution becomes more viscous and increasingly elastic, where the friction factor is not affected. Hence a minimum concentration of polymer is needed to achieve the friction factor reduction, which mainly depends on the viscosity of the solution (water-polymer solution). By increasing the concentration of DRA, the amount of friction between solid-liquid interfaces will be reduced significantly. The variation in the friction factor in the presence of DRA depends on the flow regime. A significant reduction in the friction factor was observed at low gas-liquid flow rates, i.e., under trickle flow regime. In trickle flow regime, the liquid trickles over the packing, and the presence of DRA in the liquid forms a fine coating over the packing, leading to a sharp decrease in the friction factor. But, for the case of pulse flow and dispersed bubble flow regimes, the column is under turbulent condition, where the viscous effect is not predominant and the friction reduction is very minimum.

The present experimental data, obtained using the air-water+xanthan system, were compared with the other systems (air-water, air-glycerol, air-ethylene glycol [9]). From the graph (Fig. 9) it was observed that the addition of DAR to the air-water system followed the same trend as that of other systems. In the present study, a particle size of 0.01605 m was used to analyze the friction factor with respect to the velocity of the liquid. The trend was supported by the fact that the viscous effect predominates in glycerol and ethylene glycol systems. Very low values of friction factor were obtained for the air-water+xanthahan gum system, as xanthan gum offers a smooth surface for frictionless flow over solid particles. Those long chain polymer solutions, even in lower concentration, interact with the frictional impact of fluid on solid surface due to its elongational

Fig. 7. Effect of Reynolds number on friction factor for air-water system at different L (Kg/m²s).
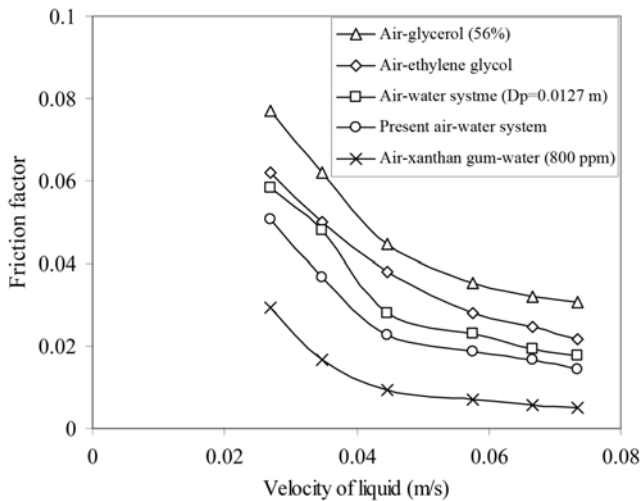
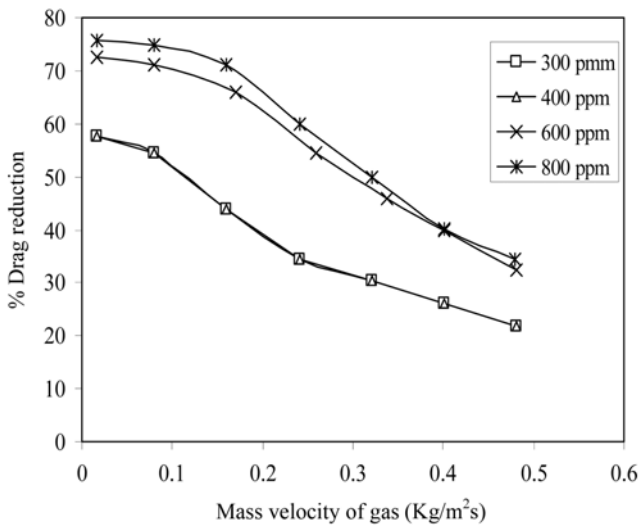Fig. 9. Effect of liquid property on friction factor.

Fig. 10. Effect of xanthan concentration on percentage drag reduction at different G (Kg/m²s).

behavior, thus reducing the friction.

4. Percentage Drag Reduction

4-1. Effect of DRA Concentration on Percentage Drag Reduction

Fig. 10 depicts the percentage reduction versus gas mass velocity through the column for a desired concentration of the xanthan gum. For the case of 300 and 400 ppm a similar effect on drag reduction was observed. This corresponds to the maximum drag reduction of 58%. For 600 ppm the maximum percentage drag reduction was quantified as 73%.

In the present study, maximum percentage of drag reduction was observed for xanthan gum concentration of 800 ppm in water. Xanthan gum as a drag reducing agent is effective for the packed bed column in the concentration range of 300 ppm to 800 ppm. Beyond 800 ppm the reverse effect is observed as drag on solid surfaces increases by increasing the concentration of xanthan gum. So by increasing the xanthan gum concentration from 300 ppm to 800 ppm, the percentage drag reduction also increases. These observa-

tions are in good agreement with those of Tiederman et al. [16]. Tiederman et al. [16] concluded that the polymer solution inhibited the formation of low speed streaks and thus drag reduction increased with polymer concentration.

4-2. Effect of Reynolds Number on Percentage Drag Reduction

The present study shows that an increase in Reynolds number increases the percentage drag reduction as reported by Mowla et al. [17]. The polymer solutions show relatively small drag reduction at low Reynolds numbers and increasingly large reduction at high Reynolds numbers. The flexible polymer molecule needs to be elongated by a large velocity gradient before its full drag reducing ability is developed [15]. This could be the reason behind the maximum drag reduction corresponding to the high liquid mass velocity. The variations in the flow patterns also confirm the observed results.

4-3. Effect of Fluid Mass Velocities on Percentage Drag Reduction

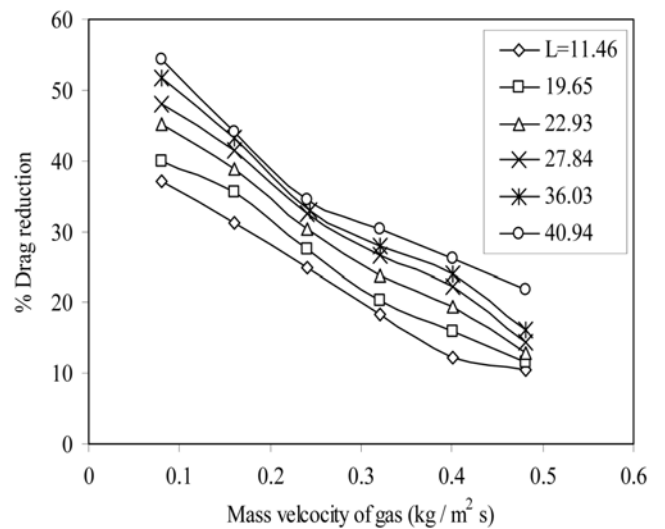Fluid viscosity is the critical factor for drag reduction in a packed

Fig. 11. Effect of mass flow rate of liquid on percentage drag reduction at different G (Kg/m²s) for 300 ppm-xanthan.
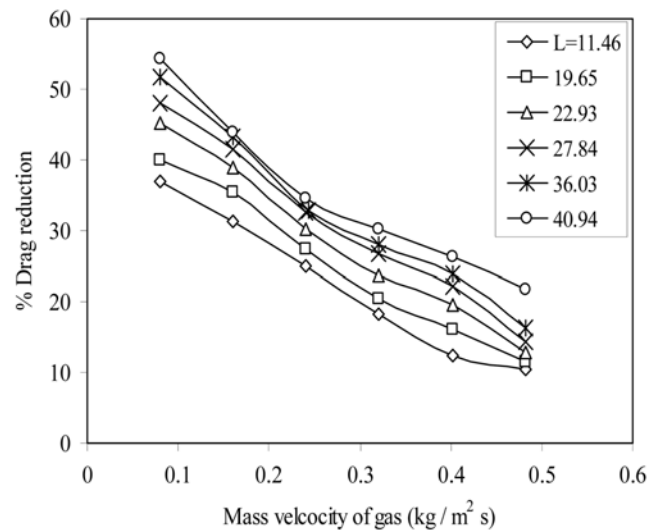

Fig. 12. Effect of mass flow rate of liquid on percentage drag reduction at different G (Kg/m²s) for 400 ppm-xanthan.
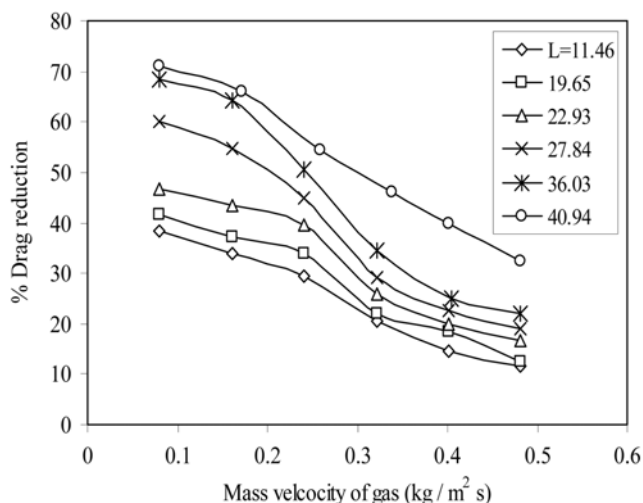
Fig. 13. Effect of mass flow rate of liquid on percentage drag reduction at different G (Kg/m²s) for 600 ppm-xanthan.
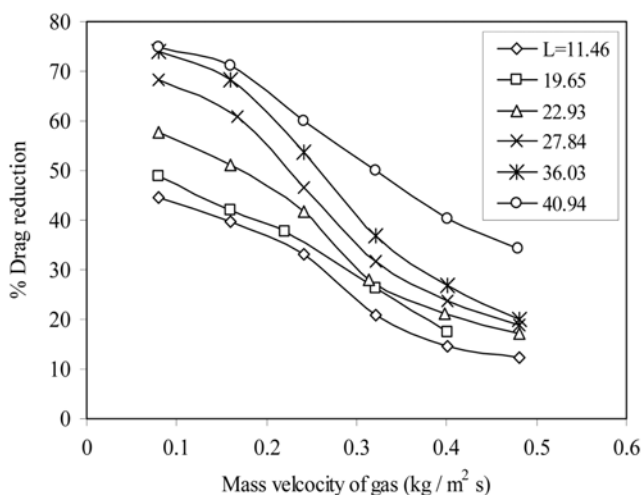

Fig. 14. Effect of mass flow rate of liquid on percentage drag reduction at different G (Kg/m²s) for 800 ppm-xanthan.

bed column. By keeping liquid mass velocity as constant and increasing gas mass velocity, the percentage drag reduction decreases (Figs. 11-14). Figs. 11 and 12 depict the percentage drag reduction versus gas mass velocity for constant liquid mass velocity for xanthan gum concentration of 300 ppm and 400 ppm, respectively. Fig. 13 shows the percentage drag reduction against gas mass velocity for xanthan gum concentration of 600 ppm. A maximum of 76% on drag reduction is observed for liquid mass velocity of 41 kg/m²s and gas mass velocity of 0.08 kg/m²s corresponding to the polymer concentration of 800 ppm. A minimum of 12.4% on drag reduction is observed for liquid mass velocity of 11.46 kg/m²s and gas mass velocity of 0.48 kg/m²s. Dukler and Hubbard [18] reported that for a constant superficial liquid velocity and DRA concentration, the total drag reduction dropped from 82% to 28% as a result of increasing superficial gas velocity.

As the mass velocity of gas increases, the interfacial force of attraction increases and the viscosity of liquid along with the DRA is not sufficient to hold the interfacial tension, leading to a decrease
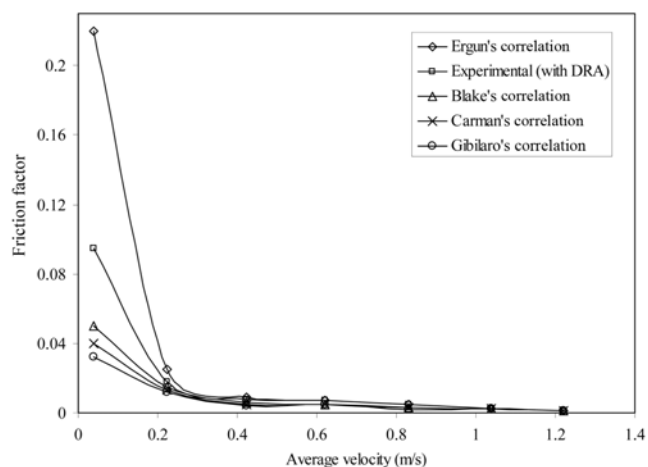

Fig. 15. Comparison plot of present experimental and literature correlations.

in the percentage drag reduction. But increasing the liquid mass velocity of polymer solution creates a smooth surface on solid particles for flow past the solid surface and also it damps eddies created near the surface. The drag reduction is sensitive to the gas and liquid superficial velocities and the particle shape and size, which are in good agreement with the observations of Al-sarkhi et al. [6,7] studies. Al-sarkhi et al. [6,7] confirmed that maximum drag reduction was achieved in the case of low superficial gas velocity and the highest superficial liquid velocity. Jourdan et al. [19] also reported maximum drag reduction for lower limits of gas velocity and for higher liquid velocity.

The friction factors obtained from the present experimental study were compared with the predicted values using available literature correlations. Fig. 15 shows the comparison for friction factor calculated using various available correlations. Friction factor calculated using various available correlations deviates much from the experimental friction factor values, which is shown in the graph (Fig. 15). The literature correlations used in the present study are listed below [20-23].

Blake's correlation is given by,

$$f_B = \frac{\Delta P \varepsilon^3}{L \rho_l (D_p)^n V^{2-n} g(1-\varepsilon)} \tag{8}$$

Carman's correlation is given by,

$$f_C = \frac{5}{Re_M} + \frac{0.4}{Re_M^{0.1}} \tag{9}$$

Carman also found that the for laminar flow, when $Re_M \leq 2$, the second term of the Carman's equation becomes negligible. The famous Ergun correlation is given by,

$$f_E = \frac{\Delta P \varepsilon^3}{L \rho_l (D_p)^n V^{2-n} g(1-\varepsilon)} = \frac{150(1-\varepsilon)}{Re_M} + 1.75 \tag{10}$$

Gibilaro's correlation is given by,

$$f_G = \frac{\Delta P \varepsilon^{4.8}}{L \rho_l (D_p)^n V^{2-n} g(1-\varepsilon)} = \frac{17.3}{Re_M} + 0.336 \tag{11}$$

From the graph (Fig. 15), it was observed that the Ergun equation

over-predicts the friction factor irrespective of the flow regime, whereas the Blake, Carman and Gibilaro correlations under-predict the friction factor for the present experimental data in trickle flow regime, since the correlations were well applicable for higher Reynolds numbers. It is also clear that all existing correlations fail to predict the friction factor at higher mean velocity. The Gibilaro correlation is promising for some range of experimental friction factor at moderate to higher Reynolds numbers, but it deviates for a wide range of friction factor at lower Reynolds number [23].

CONCLUSION

Xanthan gum is an effective drag reducing agent used in the present co-current down-flow packed column. A maximum of 76% on drag reduction was observed for a liquid mass velocity of 41 kg/m^2s and a gas mass velocity of 0.08 kg/m^2s corresponding to the polymer concentration of 800 ppm. Maximum drag reduction is observed for highest liquid velocity and low gas velocity. Due to the drag reduction by xanthan gum the flow regime transition was altered for the air-xanthan gum water system, even for very low concentrations of xanthan gum. The xanthan gum in water (solution) showed relatively less drag reduction at low Reynolds numbers and increasingly large reduction at high Reynolds numbers. Xanthan gum as drag reducing agent is effective for the present packed column in the concentration range of 300 ppm to 800 ppm. Maximum reduction in drag coefficient was observed for 800 ppm. Beyond this concentration the variation in the drag coefficient is reduced, since the variation in the liquid properties reaches a constant value.

NOMENCLATURE

D_c : diameter of column [m]
D_p : diameter of particle [m]
f_B : friction factor by Blake's correlation [-]
f_C : friction factor by Carman's correlation [-]
f_E : friction factor by Ergun's correlation [-]
f_G : friction factor by Gibilaro's correlation [-]
G : gas mass velocity [kg/m^2s]
g : acceleration due to gravity [9.81 m/s^2]
K : flow consistency index [kg/m s^{2-n}]
L : liquid mass velocity [kg/m^2s]
n : flow behavior index [-]
Re_M : modified reynolds number [-]
V : superficial velocity [m/s]
V_g : velocity of liquid through the column [m/s]
V_l : velocity of gas through the column [m/s]
X, Y and ψ : dimensionless parameters [-]
ρ_l : density of liquid [kg/m^3]
ρ_w : density of water [kg/m^3]
ΔP : pressure drop in testing section [N/m^2]
ΔP_w : pressure drop for the given length of testing section for pure water

ΔP_{DRA} : pressure drop for the system with DRA with the same flow rate of water
φ_s : sphericity [-]
σ_l : surface tension of liquid [N/m]
σ_w : surface tension of water [N/m]
μ_l : viscosity of liquid [kg/ms]
μ_w : viscosity of water [kg/ms]
ε : voidage [-]

REFERENCES

1. B. A. Toms, *Process International Rheological Congress II & III*, 135- 41, 47-9, 51-2 (1949).
2. V. T. Truong, *Drag reduction technologies*, DSTO Aeronautical and Maritime Research Laboratory, Australia (2001).
3. J. L. Lumley, *Physics Fluids.*, **20**(10), 64 (1977).
4. J. L. Lumley, *Ann. Rev. Fluid Mechanics*, **1**, 367 (1969).
5. M. R. Hanna, W. Kozicki and C. Tiu, *Chem. Eng. J.*, **13**, 93 (1977).
6. A. Al-Sarkhi, E. Abu-Nada1 and M. Batayneh, *Advances in Fluid Mechanics WIT Transactions on Engineering Sciences*, **52**, 1743 (2006).
7. A. Al-Sarkhi and A. Soleimani, *European Federation Chem. Eng.*, 1583 (2004).
8. H. Choi, P. Moin and J. Kim, *J. Fluid Mechanics*, **262**, 75 (1994).
9. P. E. JagadeeshBabu, *Ph.D. Thesis*, A.C. Tech., Anna University (2005).
10. M. E. Trivizadakis, D. Giakoumakis and A. J. Karabelas, *Chem. Eng. Sci.*, **61**, 5534 (2006).
11. J. C. Charpentier and M. Favier, *AIChE J.*, **21**(6), 1213 (1975).
12. B. I. Morsi, N. Midous and J. C. Charpentier, *AIChE J.*, **24**(2), 357 (1978).
13. D. R. Oliver and S. I. Bakhtiyarov, *J. Non-Newtonian Fluid Mechanics*, **12** 113 (1983).
14. K. Rupesh Reddy and B. Jyeshtharaj Joshi, *Chem. Eng. Res. Design*, **86**(5), 444 (2008).
15. M. P Tulin, *Proceedings of the 3rd International Conference on Drag Reduction* (1984).
16. W. G. Tiederman, T. S. Luchik and D. G. Bogard, *J. Fluid Mechanics*, **156**, 419 (1985).
17. D. Mowla and A. Naderi, *Chem. Eng. Sci.*, **61**, 1549 (2006).
18. A. E. Dukler and M. G. Hubbard, *Ind. Chem. Fundam.*, **14**(4), 337 (1975).
19. L. Jourdan, Y. Knapp, F. Oliver and J. P. Guibergia, *J. Mechanics Fluids*, **17**, 105 (1998).
20. J. W. Hoyt, *Encyclope dia of polymer science and engineering*, 5, Wiley, New York, 129 (1986).
21. J. W. Hoyt, *ASME J. Basic Eng.*, **94**, 258 (1972).
22. D. Bonn, Y. Amarouchene, C. Wagner, S. Douady and O. Cadot, *J. Physics*, **17**, 1195 (2005).
23. T. Min, J. Y. Yoo, H. Choi and D. D. Joseph, *J. Fluid Mechanics*, **486**, 213 (2003).